Sandra Pavón[1,2,*]

Maria Martínez[3]

Javier Giménez[3]

Joan de Pablo[3,4]

Se(IV) Immobilization onto Natural Siderite: Implications for High-Level Nuclear Waste Repositories

Sorption processes of metals and semimetals on siderite are studied because of its potential adequacy for removing contaminants from natural waters and its wide availability, as well as its capacity to reduce the oxidation state of some contaminants such as selenium. In this work, it has been demonstrated that siderite reduces selenite ions in solution, showing a higher selenium immobilization capacity compared to other iron(III) minerals, which is probably due to both sorption and reduction processes.

1   Introduction

Fission-based nuclear energy is nowadays a reliable power source which arises as a consequence of the reduced availability of fossil fuels as well as to counter the threat of climate change [1, 2]. Consequently, a large amount of long-term nuclear waste had been produced because of the subsequent increase of elements processing to be used in fuel and weapons [3, 4]. Hence, their mining and extraction have been spread throughout Europe becoming the disposal of the subsequent nuclear waste a crucial issue. European nuclear reactors may produce 6.6 million m^3 of nuclear waste, and over 60 000 t of spent nuclear fuel are in storage [5], being indispensable to ensure the safety management of radioactive waste owing to its potential hazard and high influence on public health [6]. Focus is required on the safe disposal and manage of spent fuel from nuclear power plants or from the non-power related use of radioactive materials for medical, industrial, agricultural, and research purposes.

Depending on the precedence of this waste, it can be classified as low-level, medium-level or high-level nuclear waste (HLNW). The last one is produced by nuclear reactors and although it contributes to < 1 % of volume of all radioactive waste, it accounts for > 95 % of the total radioactivity produced in the nuclear power process. However, no country in the world has a final disposal site for this kind of waste in operation, yet [5].

Long-lived fission products are generated in the nuclear power plants. In particular, selenium is an element of special concern in the nuclear fuel cycle, and it is one of the main radionuclides considered in the safety analysis of a high-level nuclear waste repository (HLNWR), because of the long half-life [79]Se isotope, which is chemically and radiologically toxic [7]. Selenium has a toxicity at concentrations > 1 mg kg^{-1} of body weight [8] and the maximum contaminant level (MCL) in drinking water is < 50 μg L^{-1} [9]. In addition, the [79]Se isotope is a highly mobile element in oxidizing geochemical environ-

ments and may have a high impact on the cumulative radioactive dose if there is not a mechanism that might retard its transport through the geosphere [10]. Its high mobility in aqueous environments is due to the fact that both Se(IV) and Se(VI) predominate in solution as anionic species in a wide pH range. Furthermore, the nuclear process is not the only anthropogenic selenium source in the environment, it is also produced in activities related to agriculture and combustion of fossil fuels [11].

In this regard, finding different adsorbents which are able to retard its presence in the biosphere and thus, contributing to a greener environment, is a promising challenge. In recent years, Fe-oxides have been extensively demonstrated as potential adsorbents for various radionuclides. In particular, goethite, hematite, and magnetite can effectively decrease the concentration in solution of a wide range of radionuclides [12–15].

Siderite ($FeCO_3$) is one of the most abundant Fe(II)-bearing carbonate minerals present in geological formations [16]. It has been found widely distributed in China, Canada, Austria, and Russia [17]. Moreover, it is a relatively cheap material which is

[1]Dr. Sandra Pavón
sandra.pavon-regana@chemie.tu-freiberg.de
TU Bergakademie Freiberg, Institute of Chemical Technology, Leipziger Str. 29, 09599 Freiberg, Germany,

[2]Dr. Sandra Pavón
Universitat Politècnica de Catalunya, Chemical Engineering Department, Diagonal 647, 08028 Barcelona, Spain.

[3]Dr. Maria Martínez, Dr. Javier Giménez, Dr. Joan de Pablo
Universitat Politècnica de Catalunya, Chemical Engineering Department and Barcelona Research Center in Multiscale Science and Engineering, Eduard Maristany 10–14, 08930 Barcelona, Spain.

[4]Dr. Joan de Pablo
Fundació CTM Centre Tecnològic, Plaça de la Ciència 2, 08243 Manresa, Spain.

being tested as a material for removing contaminant species from wastewater, drinking water or aquatic weed plants, such as As [9, 16, 18], Pb^{2+} [19], Hg^{2+} [20], and U [21]. Different studies were carried out to establish the sorption capacity of siderite for different contaminants, mainly arsenic [22–24], because of the importance of its presence in waters. Furthermore, it was not known that carbonate minerals could absorb anionic species, and arsenic is found mostly as oxyanions in natural waters [25].

The main conclusion of those studies was that siderite also had a high sorption capacity for arsenic (higher for arsenic(III) than for arsenic(V)). Siderite is assumed to be also formed as a secondary solid phase during the reductive dissolution of iron(III) (hydr)oxides by organic matter and bacteria under anaerobic conditions [26–28]. This process could be critical from the environmental point of view because the contaminants previously sorbed onto the high-sorption capacity iron(III) (hydr)oxides could be released to the waters.

The few studies carried out on the interaction of selenite ion with siderite were mainly devoted to the possible surface redox reactions, because of the possible oxidation of Fe(II) on the surface of siderite and the reduction of selenium in solution or sorbed onto the siderite surface. Under strictly anoxic conditions, the reduction of a percentage of Se(IV) to Se(0) was demonstrated by time-resolved X–ray near-edge absorption spectroscopy and X-ray absorption [29, 30]. Under such redox conditions, the reduction of Se(IV) together with its sorption on the solid surface indicated promising siderite properties for the immobilization of selenium in an HLNWR.

The main purpose of this research was to determine the capacity of a natural siderite to decrease selenium(IV) mobility in a contaminated environment. A natural siderite was used instead of synthetic siderite to work with a solid closer to the ones present in a natural system. By means of experiments where the variation of Se(IV) concentration in solution was measured after the contact with the solid, the capacity of siderite to hinder Se(IV) mobility in the solution was discussed considering that the mechanism of Se(IV) incorporation to the solid is probably not only based on sorption, but redox reactions on the solid surface such as the reduction of Se(IV) to Se(0) should not be discarded and, actually, might represent a beneficial mechanism to decrease selenium concentration in solution [29]. The determination of the sorption capacity of the mineral will allow evaluating its potential capacity to retard the migration of selenium to the environment, contributing to the nuclear wastewater management to promote a safer environment.

2 Materials and Methods

2.1 Characterization of the Natural Siderite

The source of the siderite used in the current research is placed in Bordes de Conflent (Lleida, Spain). The original solid was crushed and sieved obtaining a particle size range from 0.075 to 0.106 µm. The siderite mineral was characterized by X-ray diffraction (XRD; Bruker D8 Advance) using a Cu X-ray tube, 40 kV, 40 mA with an opening angle of 5° 2θ. The X-ray tube

was operated at 30 kV and 10 mA. The XRD patterns were collected with a step of 0.02° and 1 s dwell time.

The surface area of the mineral with a 0.075–0.106 µm particle size was determined by the Brunauer-Emmett-Teller (BET) methodology using $N_2(g)$ as adsorbed gas by a FlowSorb 2300 (Micromeritics Instrument Corp., USA).

The point of zero charge of the solid (pH_{pzc}) was determined by using the so-called immersion methodology [31]. An amount of 0.05 g of siderite was immersed in 10 cm^3 of a 0.1 mol L^{-1} NaCl (Ref. 131659, PanReac AppliChem) solution with a known initial pH (5–10, measured with a GLP-22 Crison 50-14 pH-meter). The equilibrium pH (pH_{eq}) was determined after 24 h of contact. The variation of the pH against initial pH showed a V-shaped curve, with the vertex of the V curve indicating the pH at which surface positive and negative charges are equal.

2.2 Sorption Procedure

Selenium solutions used in the experiments were prepared by dissolving Na_2SeO_3 (Ref. 2114485, supplied by Sigma-Aldrich) in Milli-Q water. Sorption batch experiments were carried out under anoxic conditions at room temperature and using the same procedure reported in previous work [25]. A portion of 0.1 g of siderite was introduced to 20 cm^3 of selenium solution in stoppered polystyrene tubes. The tubes were continuously stirred at 30 rpm using an RM-2M Intelli-Mixer (ELMI, USA) and centrifuged at 6100 rpm for 4 min by a Centronic BL-II (JP-Selecta, Spain). Samples were filtered through 0.22-µm pore size filters. Selenium and iron concentrations in solution were measured by inductively coupled plasma mass spectrometry (ICP-MS; Model 7850, Agilent Technologies, USA). The concentration of Se attached to the solid (Q_e)[1]) in mol g^{-1} and the percentage of Se eliminated from the solution (%$Se_{removed}$) were determined by Eqs. (1) and (2):

$$Q_e = \frac{[Se]_0 - [Se]}{m_{FeCO_3}} V \qquad (1)$$

$$\%Se_{removed} = \left(\frac{[Se]_0 - [Se]}{[Se]_0}\right) \cdot 100 \qquad (2)$$

where $[Se]_0$ and $[Se]$ are the initial and final selenium concentrations (mol dm^{-3}), m_{FeCO3} is the amount of the siderite (g), and V is the volume of the dissolution (m^3).

The pH of the solutions was varied by adding some drops of either concentrated HCl (Ref. AC07371000, Scharlau) or NaOH (Ref. 131687, PanReac AppliChem) and waiting until the new pH value was constant. The ionic medium was 0.1 mol dm^{-3} NaCl in all the experiments.

---

1)   List of symbols at the end of the paper.

2.2.1 Kinetics

The study on the sorption kinetics was carried out in order to know on the one hand the equilibrium time, which was used in subsequent series of experiments, and on the other hand if the kinetics of the process was critical for the immobilization of contaminant selenium(IV) onto siderite.

The variation of the selenium sorption with time was carried out using 0.1 g of siderite in contact with a solution of 6.27×10^{-5} mol dm^{-3} selenium(IV) at initial pH 7.4. Different aliquots were taken from the solution along time.

The study of the kinetic modeling was performed by using the linearized pseudo-second-order rate equation [32], which is depicted in Eq. (3):

$$\frac{t}{Q_t} = \frac{1}{k_2 \cdot Q_e^2} + \frac{1}{Q_e} t \qquad (3)$$

where Q_t and Q_e are sorbed amounts at time t and at equilibrium (mol Se(IV) g^{-1} siderite), t is contact time (h), and k_2 is the pseudo-second-order rate constant (g mol^{-1}h^{-1}).

2.2.2 Isoterms

Solutions with different initial selenium(IV) concentrations from 1.2×10^{-5} to 6.3×10^{-4} mol dm^{-3}, were mixed with 0.1 g of siderite for 24 h. Two different series of experiments were carried out, which differed on the initial pH (7.1 and 8.0).

The experimental data were fitted by means of the most utilized empirical models, i.e., Langmuir and Freundlich. The Langmuir isotherm assumes that on the surface of an adsorbent there is a monolayer containing a finite number of sorption sites, while the Freundlich isotherm explains the multilayer sorption onto the heterogeneous surface of adsorbent [33]. The Langmuir isotherm model is given as follows [32]:

$$Q_e = \frac{Q_{max} K_L [Se]_{eq}}{1 + K_L [Se]_{eq}} \qquad (4)$$

where Q_{max} is the maximum sorption capacity (mol g^{-1}), K_L is the Langmuir constant (dm^{3}mol^{-1}), $[Se]_{eq}$ is the equilibrium selenium concentration (mol dm^{-3}).

The equilibrium parameter, R_L, was also calculated by Eq. (5) [34, 35]. This parameter gives an insight on the essential characteristics of the isotherm, indicating if the process of sorption is favorable, unfavorable, or irreversible [36].

$$R_L = \frac{1}{1 + K_L [Se]_0} \qquad (5)$$

Regarding the Freundlich model, the following sorption equilibrium (Eq. (6)) describes the model [32]:

$$Q_e = K_F [Se]_{eq}^{1/n} \qquad (6)$$

where K_F is the Freundlich constant (dm^{3}mol^{-1}) and $1/n$ is a stoichiometric coefficient which controls the effective concentration of the selenium in solution.

A speciation diagram of H_2SeO_3 was generated by using MEDUSA software [37] with a Se(IV) concentration of 2×10^{-4} mol dm^{-3} to investigate which species predominate at each pH value in solution.

2.2.3 Influence of pH of the Se(IV) Sorption on Siderite

The influence of the pH value in solution for the Se(IV) sorption on siderite was evaluated by different experiments. The pH range studied was from 2.83 to 8.87. A portion of 0.1 g of siderite was introduced to 20 cm^3 of selenium solution ($[Se]_0 = 1.67 \times 10^{-4}$ mol dm^{-3} and 0.1 mol dm^{-3} NaCl). The sorption producer followed was according to Sect. 2.2 and the Se(IV) absorbed (Q_e) was determined by Eq. (1).

3 Results and Discussion

3.1 Characterization of the Natural Siderite

The XRD pattern from the siderite is very similar to the siderite reference pattern (Fig. 1). The characteristic peaks in 25.02, 32.09, 42.66, 46.35, and 53.04 2θ are found in both patterns. Thus, the mineral was confirmed to be mainly siderite by using XRD and no other solid phases were detected, although these could be present in relatively low quantities.
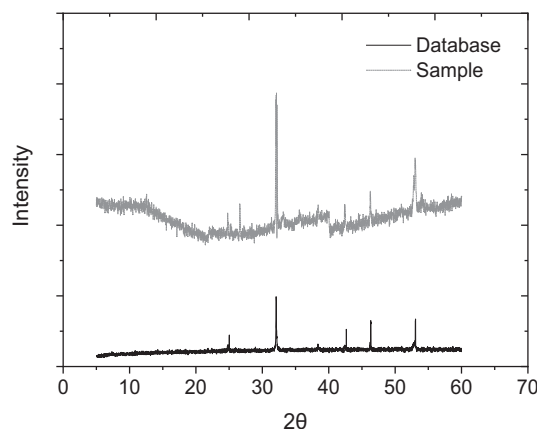

Figure 1. XRD patterns of siderite (FeCO$_3$).

The surface area obtained by applying the BET method was 7.57 ± 0.02 m^{2}g^{-1}. The value was similar to that obtained in another investigation [38] but it was considerably higher than that obtained for other iron minerals, being ~ 4 and ~ 20 times higher than for goethite and hematite, respectively [39]. This result is promising, considering siderite as the best one to immobilize Se(IV) compared to the other previous iron minerals.

In order to find the pH value at which the apparent surface charge density of the natural siderite in the presence of an inert electrolyte is not dependent on the ionic strength, the immersion methodology was carried out. The results are depicted in Fig. 2 and the pH$_{pzc}$ of the solid was 7.2 ± 0.1, similar to 7.4–7.9, which were the values determined for siderite in other studies [40].
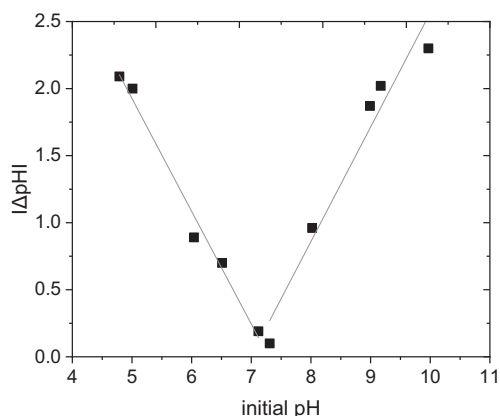
Figure 2. Variation of the equilibrium pH as a function of initial pH in the immersion experiments with 0.05 g of siderite (0.1 mol dm^{-3} NaCl as ionic medium).

3.2 Sorption

3.2.1 Kinetics

The retention percentages were very high for the whole time range studied (0.08–24 h) achieving retention values > 88 % after 5 min (Tab. 1). Hence, the Se sorption rate in siderite is faster compared to other systems such as FeOOHs or nanocrystalline magnetite because the equilibrium is reached after 30 min instead of 4 h and 7 days, respectively [41, 42].

Table 1. Se(IV) sorption onto siderite as a function of time (0.1 g siderite, pH$_0$ = 7.4, [Se]$_0$ = 6.27×10^{-5} mol dm^{-3}, 0.1 mol dm^{-3} NaCl).

Time [h]	pH$_{eq}$	$Q_e \times 10^5$ [mol g^{-1}]	Se$_{removed}$ [%]
0.08	7.29	1.11	88.08
0.30	7.19	1.09	92.53
0.50	7.03	1.09	95.35
0.75	7.03	1.11	95.35
1	6.98	1.16	95.75
2	6.95	1.19	94.34
24	7.83	1.19	94.14

Sorption onto natural siderite was also faster than the sorption of selenite ion on other iron(III) natural minerals such as goethite, hematite, and magnetite, where the equilibrium was reached in some hours or days [39, 43]. Thus, the sorption of Se(IV) on siderite will not be kinetically controlled. On the other hand, similar results were obtained for the sorption of arsenic oxyanions on synthetic siderite, where the equilibrium was reached after 120 min, faster than on other iron(III) solids [22, 24].

Furthermore, iron concentrations in solution were also determined in order to account for the potential siderite disso-

lution, although the solubility at the experimental pH values was expected to be very low [44]. Iron concentrations were always lower than 3×10^{-7} mol dm^{-3} (detection limit (DL) of the ICP-MS), confirming the low siderite solubility, in contrast with experiments with synthetic siderite [29]. At such low iron concentrations, redox reactions in solution between selenium and aqueous Fe(II) seem to be negligible, which does not preclude reduction of selenium(IV) to selenium(0) on the surface of siderite.

The modeling of the kinetic data was carried out to describe the sorption of selenium(IV) on siderite under the studied experimental conditions. As depicted in Fig. 3, the sorption process follows a pseudo-second-order kinetics due to the best fitting of the model to the experimental data ($R^2 > 0.9999$). The rate constant of sorption obtained is 3.44×10^5 g mol^{-1}h^{-1}, and 1.19×10^{-5} mol g^{-1} is the Se(IV) sorbed (94.34 %) at equilibrium.

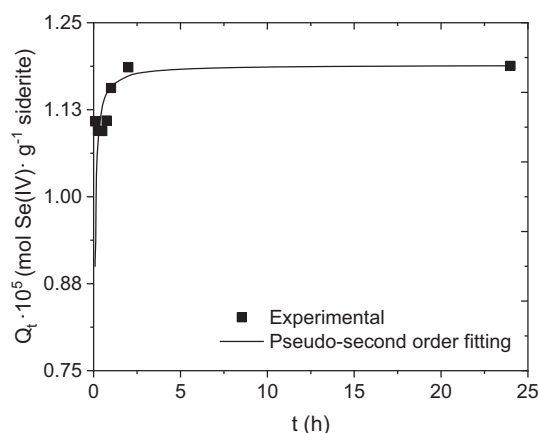**Figure 3.** Kinetics of selenium(IV) sorption onto siderite; 0.1 g of siderite, 6.27×10^{-5} mol dm^{-3} of Se(IV) in 0.1 mol dm^{-3} NaCl at pH 7.4.

Although the initial Se(IV) concentration was similar for the kinetic experiments with goethite, hematite, magnetite, and siderite, the rate constants obtained are similar when magnetite and siderite are used [39, 43]. However, comparing these rate constants to those found in the experiments with goethite and hematite, they are considerably higher. Furthermore, the amount of Se(IV) sorbed at equilibrium is higher when the iron mineral is siderite instead of goethite, hematite or magnetite. The increase on the sorption rate in solids with structural Fe(II) points to the possibility that the likely reduction of selenium(IV) at the surface of the solids (in siderite and magnetite) affects the kinetics of the reduction of selenium in solution.

3.2.2 Isotherms

The adsorption isotherms including Langmuir and Freundlich isotherms models were widely used to establish the amount of Se(IV) adsorbed onto siderite. The selenium(IV) sorbed as a function of the selenium concentration remaining in solution at equilibrium is shown in Fig. 4. To better understand the
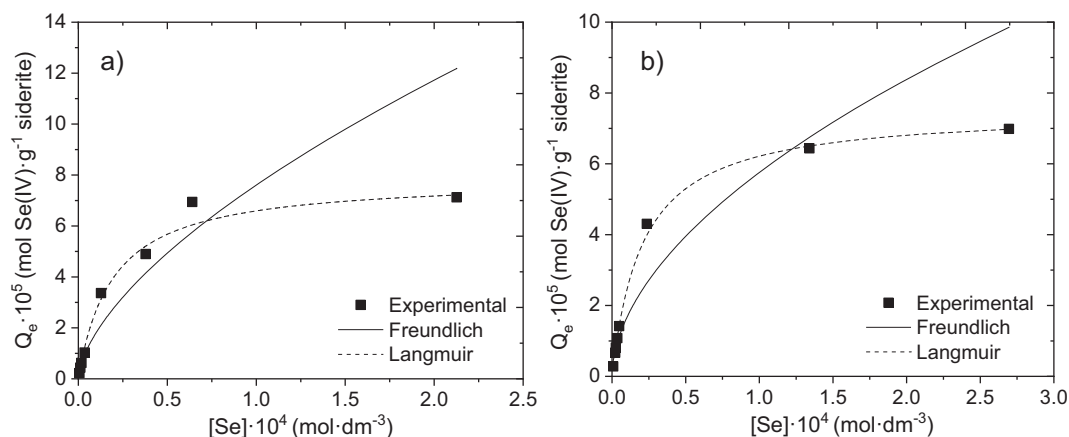
Figure 4. Adsorption isotherms of Se(IV) at equilibrium at (a) pH 7.1 ± 0.7, (b) pH 8.0 ± 0.7; 0.05 g of siderite (0.1 mol dm^{-3} NaCl as ionic medium).

adsorption process, experimental data were fitted to both models. The good fitting of the data to the Langmuir model for both duplicates is obvious (Fig. 4). The correlation coefficients (R^2) for the Freundlich model were 0.9445 and 0.9330 at pH 7.1 and 8.0, respectively, whereas the R^2 values for the Langmuir model were 0.9978 and 0.9999.

The experimental data fitting to the Langmuir model gave the parameters K_L and Q_{max} as well as the sum square of residuals (SSR) values as summarized in Tab. 2.

Table 2. Parameters obtained for the fitting of the Langmuir isotherm to the sorption of selenium(IV) onto siderite.

Initial pH	K_L [dm^{3}mol^{-1}]	Q_{max} [mol g^{-1}]	SSR[a]
7.1	5.15×10^4	7.87×10^{-5}	1.34×10^{-8}
8.0	4.75×10^4	7.52×10^{-5}	1.11×10^{-8}

[a] SSR: sum square of residuals.

The fitting of the Langmuir isotherm to the experimental sorption data indicates that the main process for the reduction of selenite ions in solution would be its sorption on siderite via monolayer coverage of the solid surface. The same model was previously deduced for the sorption of Se(IV) onto hydrous iron oxides [39, 43, 45]. However, once more the possibility of redox reactions at the surface of the solid should not be discarded, although the reduction process could mainly affect the sorbed selenium(IV).

The results obtained at both pH values are very similar, indicating that the main sorption mechanism is not based on electrostatic interactions because at both pH values the selenium(IV) species in solution are the oxyanions SeO$_3^{2-}$ and HSeO$_3^-$ (Fig. 5), whose sorption, assuming an electrostatic mechanism for sorption, would be lower at pH > pH$_{pzc}$ (surface of the solid negatively charged) than at a pH similar to pH$_{pzc}$ (surface of the solid not charged).

Furthermore, the R_L parameter was also determined from the Langmuir isotherm modeling results by using Eq. (5). If $0 < R_L < 1$, the sorption process is favorable, while higher values indicate that it is unfavorable. Fig. 6 illustrates the variation of R_L with initial selenium(IV) concentration in solution.

R_L parameter values are always < 1, especially at higher selenium concentrations, indicating that the sorption of selenium(IV) onto siderite is favorable under the experimental conditions studied.

3.2.3 Influence of pH and Comparison of the Sorption on Siderite with Iron Oxides and Hydroxides

The variation of the pH of the solution observed in the experiments for the pH$_{pzc}$ determination already demonstrated that the solid was able to buffer the pH to values near the pH$_{pzc}$, due to the own acid-base properties of the solid. A similar buffer behavior was observed when selenium was present in the solution because the pH$_{eq}$ was almost constant except when
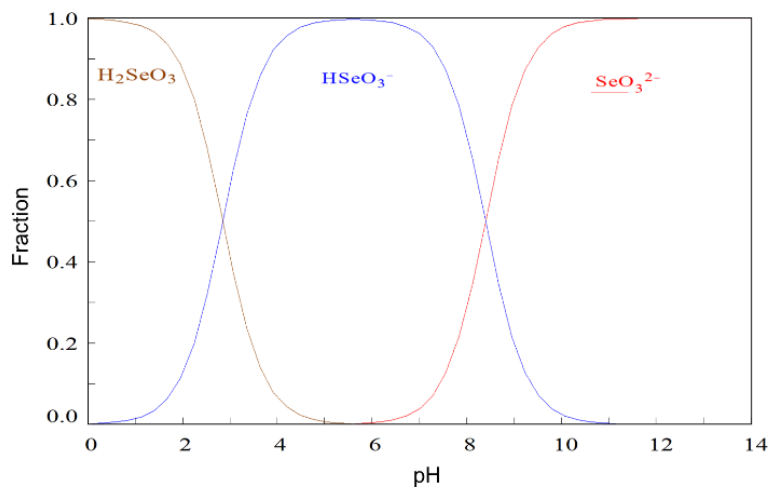

Figure 5. Speciation diagram using MEDUSA software [37]. [Se(IV)] = 2×10^{-4} mol dm^{-3}.
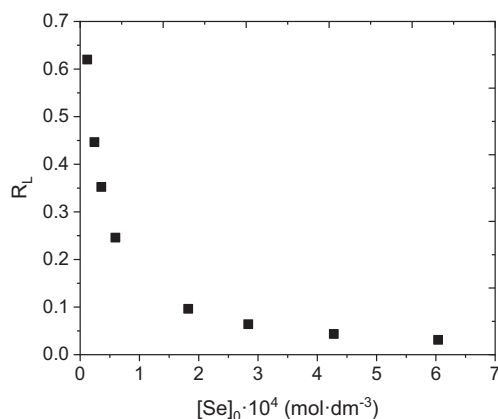
Figure 6. Variation of the R_L parameter with initial selenium(IV) concentration in solution.

the initial pH was strongly acid. In Tab. 3 it can also be seen that the retention was highly constant in the initial pH range studied.

Table 3. Influence of the pH in the experiments of selenium(IV) sorption on siderite for 24 h (0.1 g siderite, $[Se]_0 = 1.67 \times 10^{-4}$ mol dm^{-3}, 0.1 mol dm^{-3} NaCl).

$pH_{initial}$	pH_{eq}	$Q_e \times 10^7$ [mol g^{-1}]
2.83	4.82	5.72
3.97	6.15	5.57
5.16	6.36	5.05
5.91	6.54	5.30
6.64	6.71	5.56
7.41	6.89	4.98
7.94	7.02	5.06
8.87	7.05	5.05

The iron concentrations in solution were always lower than the DL of the analytical technique, indicating that the dissolution of the natural siderite under these conditions was also negligible. Once more, the speciation of selenium in solution is probably not affected by the release of such low iron concentrations.

As mentioned above, the slow variation of the sorption at pH values higher and lower than the point of zero charge points to a nonelectrostatic mechanism. The same behavior was observed in the case of the removal of arsenic using siderite, with different mechanisms proposed such as electrostatic interaction, surface complexation, and specific adsorption [16]. Although in the case of arsenic sorption onto siderite an important effect of pH was claimed by Guo et al. [46], actually, the variation of sorption is given by the authors as a function of initial pH and, as it is shown in this work and is also indicated by the authors, the equilibrium pH might be very differ-

ent from the initial pH due to the buffering capacity of the solid, increasing with the surface area. The sorption of selenite ions onto other iron minerals was already determined to be based on the formation of surface complexes, whose composition was derived from the variation of the sorption capacity with pH. The surface area of the solids was lower than that of the siderite used in this work and the pH of the solution in contact with the solids was not buffered [39, 43].

Fig. 7 presents a comparison between the sorption capacity obtained in this work with siderite and published sorption capacities for magnetite, goethite, and hematite determined with the same methodology and with the same initial selenium concentrations and weight of solid as a function of pH [39, 43].
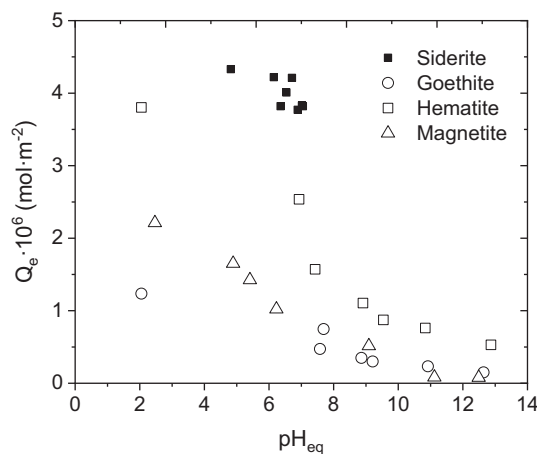

Figure 7. Variation of the sorption capacity with equilibrium pH. Data from goethite, hematite, and magnetite from [39, 43].

The sorption of selenium(IV) seems to be higher on siderite than on other iron minerals at pH values from 6 to 8 (Fig. 7). However, the higher capacity of siderite to reduce the selenium concentration in solution could also be related to the reducing properties of the solid because of the presence of structural Fe(II). Actually, the reduction of selenium to Se(0) was demonstrated by Scheinost et al. [29], who found that 60 % of selenium on the siderite surface was reduced to Se(0). However, those authors worked with a freshly synthesized siderite and it can be stated that probably the reduction of selenium is occurring, once selenium is sorbed on the solid or even at the aqueous phase in contact with the solid. In any case, the selenium concentration at the bulk solution decreased when siderite was present, which increases the beneficial properties of siderite to hinder selenium mobility in natural waters.

From the data obtained in the present work, it is obvious that the decrease of selenium determined in the experiments is higher than predicted if only sorption is considered. Rakshit et al. [47] determined the number of active sites in siderite and, considering the weight and surface area of the siderite used in our experiments, the number of active sites would be 4×10^{-6} moles at pH 7. This value is lower than the reduction of selenium observed in our experiments at the same pH considering the data of Tab. 2, namely, 8×10^{-6} mol, indicating that an amount of selenium was not related to sorption, and the decrease of

selenium in the experiments was not only due to a sorption process but also to a certain reduction of Se(IV) to Se(0).

However, it should be noted that in our work the redox state of the solid and of the selenium after the sorption process was not determined. Future analysis of the redox state could provide more information on the actual sorption capacity of siderite.

4 Conclusions

Natural siderite can be used as a reactive barrier in selenite ion polluted environments, due to its high sorption capacity for selenite ion and its fast sorption process. This fact allows contributing to a safer environment, immobilizing radioactive elements, such as the isotope ^{79}Se(IV), which remain in the nuclear waste, to delay its appearance in the biosphere.

The sorption follows a pseudo-second-order kinetics obtaining $3.44 \times 10^5 \, \mathrm{g \, mol^{-1} h^{-1}}$ as a rate constant and $1.19 \times 10^{-5} \, \mathrm{mol \, g^{-1}}$ of Se(IV) sorbed at equilibrium. The variation of the sorption onto $FeCO_3$ with the Se(IV) concentration in solution has been modeled by a Langmuir isotherm, which means that a monolayer is formed on the siderite surface.

Furthermore, the sorption capacity of siderite for selenite ion is higher than that of minerals such as hematite, goethite, and magnetite, which are characterized by incorporating oxyanions. Due to the presence of structural Fe(II) in siderite, the reduction of some selenium(IV) to selenium(0) is likely. This reduction would have a beneficial effect on the decrease of selenium mobility in the environment, due to the reduction of highly mobile selenium species to solid Se(0).

Acknowledgment

The authors have declared no conflict of interest.

Symbols used

k_2	[–]	pseudo-second-order rate constant
K_L	[$dm^3 mol^{-1}$]	Langmuir constant
K_F	[–]	Freundlich constant
pH_{pzc}	[–]	point of zero charge of the solid
pH_{eq}	[–]	equilibrium pH
Q_e	[$mol \, g^{-1}$]	concentration of Se attached to the solid
Q_{max}	[$mol \, g^{-1}$]	maximum sorption capacity
Q_t	[$mol \, g^{-1}$]	sorbed amount of Se at time t
R_L	[–]	equilibrium parameter
[Se]	[$mol \, dm^{-3}$]	final selenium concentration
$[Se]_0$	[$mol \, dm^{-3}$]	initial selenium concentration
$[Se]_{eq}$	[$mol \, dm^{-3}$]	equilibrium Se concentration
$\%Se_{removed}$	[–]	percentage of Se eliminated from the solid
SSR	[–]	sum square of residuals
t	[h]	contact time
V	[m^3]	volume of the dissolution

Abbreviations

HLNW	high-level nuclear waste
HLNWR	high-level nuclear waste repository
MCL	maximum contaminant level
XRD	X-ray diffraction

References

[1] R. Prăvălie, G. Bandoc, *J. Environ. Manage.* **2018**, *209*, 81–92. DOI: https://doi.org/10.1016/j.jenvman.2017.12.043

[2] R. Geng, W. Wang, Z. Din, D. Luo, B. He, W. Zhang, *J. Mol. Liq.* **2020**, *309*, 113029. DOI: https://doi.org/10.1016/j.molliq.2020.113029

[3] Y. Sun, X. Wang, Y. Ai, Z. Yu, W. Huang, C. Chen, T. Hayat, A. Alsaedi, X. Wang, *Chem. Eng. J.* **2017**, *310*, 292–299. DOI: https://doi.org/10.1016/j.cej.2016.10.122

[4] X. Y. Zheng, Y. H. Shen, X. Y. Wang, T. S. Wang, *Chemosphere* **2018**, *203*, 109–116. DOI: https://doi.org/10.1016/j.chemosphere.2018.03.165

[5] M. Besnard, M. Schneider, G. MacKerron, W. Neumann, A. Turmann, A. Jungjohann, *The World Nuclear Waste Report 2019*, **2019**.

[6] T. Vander Beken, N. Dorn, S. Van Daele, *J. Environ. Manage.* **2010**, *91 (4)*, 940–948. DOI: https://doi.org/10.1016/j.jenvman.2009.11.012

[7] B. Grambow, *J. Contam. Hydrol.* **2008**, *102 (3–4)*, 180–186. DOI: https://doi.org/10.1016/j.jconhyd.2008.10.006

[8] National Research Council, *Effects of Excess Selenium*, National Academy Press, Washington, DC **1983**.

[9] S. O. Adio, M. H. Omar, M. Asif, T. A. Saleh, *Process Saf. Environ. Prot.* **2017**, *107*, 518–527. DOI: https://doi.org/10.1016/j.psep.2017.03.004

[10] F. Séby, M. Potin-Gautier, E. Giffaut, O. F. X. Donard, *Analusis* **1998**, *26 (5)*, 193–198. DOI: https://doi.org/10.1051/analusis:1998134

[11] Z. Li, D. Liang, Q. Peng, Z. Cui, J. Huang, Z. Lin, *Geoderma* **2017**, *295*, 69–79. DOI: https://doi.org/10.1016/j.geoderma.2017.02.019

[12] A. C. Scheinost, L. Charlet, *Environ. Sci. Technol.* **2008**, *42 (6)*, 1984–1989. DOI: https://doi.org/10.1021/es071573f

[13] S. E. O'Reilly, D. G. Strawn, D. L. Sparks, *Soil Sci. Soc. Am. J.* **2001**, *65 (1)*, 67–77. DOI: https://doi.org/10.2136/sssaj2001.65167x

[14] M. Li, Y. Sun, H. Liu, T. Chen, T. Hayat, N. S. Alharbi, C. Chen, *ACS Sustainable Chem. Eng.* **2019**, *7 (12)*, 11035. DOI: https://doi.org/10.1021/acssuschemeng.9b01880

[15] E. S. Ilton, J. F. S. Boily, E. C. Buck, F. N. Skomurski, K. M. Rosso, C. L. Cahill, J. R. Bargar, A. R. Felmy, *Environ. Sci. Technol.* **2010**, *44 (1)*, 170–176. DOI: https://doi.org/10.1021/es9014597

[16] H. Guo, D. Stüben, Z. Berner, *J. Colloid Interface Sci.* **2007**, *315 (1)*, 47–53. DOI: https://doi.org/10.1016/j.jcis.2007.06.035

[17] Y. Yang, T. Chen, X. Zhang, C. Qing, J. Wang, Z. Yue, H. Liu, Z. Yang, *Chemosphere* **2018**, *199*, 130–137. DOI: https://doi.org/10.1016/j.chemosphere.2018.02.014

[18] F. Li, H. Guo, X. Zhou, K. Zhao, J. Shen, F. Liu, C. Wei, *Chemosphere* **2017**, *168*, 777–785. DOI: https://doi.org/10.1016/j.chemosphere.2016.10.135

[19] I. Vergili, Z. B. Gönder, Y. Kaya, G. Gürdağ, S. Çavuş, *Process Saf. Environ. Prot.* **2017**, *107*, 498–507. DOI: https://doi.org/10.1016/j.psep.2017.03.018

[20] J. Ha, X. Zhao, R. Yu, T. Barkay, N. Yee, *Appl. Geochem.* **2017**, *78*, 211–218. DOI: https://doi.org/10.1016/j.apgeochem.2016.12.017

[21] S. Srivastava, K. C. Bhainsa, *J. Environ. Manage.* **2016**, *167*, 124–129. DOI: https://doi.org/10.1016/j.jenvman.2015.11.018

[22] J. Jönsson, D. M. Sherman, *Chem. Geol.* **2008**, *255 (1–2)*, 173–181. DOI: https://doi.org/10.1016/j.chemgeo.2008.06.036

[23] K. Zhao, H. Guo, X. Zhou, *Appl. Geochem.* **2014**, *48*, 184–192. DOI: https://doi.org/10.1016/j.apgeochem.2014.07.016

[24] H. Guo, Y. Li, K. Zhao, Y. Ren, C. Wei, *J. Hazard. Mater.* **2011**, *186 (2–3)*, 1847–1854. DOI: https://doi.org/10.1016/j.jhazmat.2010.12.078

[25] J. Giménez, M. Martínez, J. de Pablo, M. Rovira, L. Duro, *J. Hazard. Mater.* **2007**, *141 (3)*, 575–580. DOI: https://doi.org/10.1016/j.jhazmat.2006.07.020

[26] A. Horneman et al., *Geochim. Cosmochim. Acta* **2004**, *68 (17)*, 3459–3473. DOI: https://doi.org/10.1016/j.gca.2004.01.026

[27] M. L. Polizzotto, C. F. Harvey, S. R. Sutton, S. Fendorf, *Proc. Natl. Acad. Sci. U. S. A.* **2005**, *102 (52)*, 18819–18823. DOI: https://doi.org/10.1073/pnas.0509539103

[28] J. M. McArthur et al., *Appl. Geochem.* **2004**, *19 (8)*, 1255–1293. DOI: https://doi.org/10.1016/j.apgeochem.2004.02.001

[29] A. C. Scheinost, R. Kirsch, D. Banerjee, A. Fernandez-Martinez, H. Zaenker, H. Funke, L. Charlet, *J. Contam. Hydrol.* **2008**, *102 (3–4)*, 228–245. DOI: https://doi.org/10.1016/j.jconhyd.2008.09.018

[30] V. Badaut, M. L. Schlegel, M. Descostes, G. Moutiers, *Environ. Sci. Technol.* **2012**, *46 (19)*, 10820–10826. DOI: https://doi.org/10.1021/es301611e

[31] N. Fiol, I. Villaescusa, *Environ. Chem. Lett.* **2009**, *7 (1)*, 79–84. DOI: https://doi.org/10.1007/s10311-008-0139-0

[32] P. Wu, Q. Zhang, Y. Dai, N. Zhu, Z. Dang, P. Li, J. Wu, X. Wang, *Geoderma* **2011**, *164 (3–4)*, 215–219. DOI: https://doi.org/10.1016/j.geoderma.2011.06.012

[33] M. Talebi, S. Abbasizadeh, A. R. Keshtkar, *Process Saf. Environ. Prot.* **2017**, *109*, 340–356. DOI: https://doi.org/10.1016/j.psep.2017.04.013

[34] V. Vadivelan, K. Vasanth Kumar, *J. Colloid Interface Sci.* **2005**, *286 (1)*, 90–100. DOI: https://doi.org/10.1016/j.jcis.2005.01.007

[35] R. Sureda, X. Martínez-Lladó, M. Rovira, J. de Pablo, I. Casas, J. Giménez, *J. Hazard. Mater.* **2010**, *181 (1–3)*, 881–885. DOI: https://doi.org/10.1016/j.jhazmat.2010.05.095

[36] E. I. El-Shafey, *J. Environ. Manage.* **2007**, *84 (4)*, 620–627. DOI: https://doi.org/10.1016/j.jenvman.2007.03.021

[37] I. Puigdomenech, *Make Equilibrium Diagrams using Sophisticated Algorithms (MEDUSA software)*, Royal Institute of Technology, Sweden **2013**.

[38] D. Shu, H. Liu, T. Chen, D. Chen, X. Zou, C. Wang, M. Li, H. Wang, *Environ. Sci. Pollut. Res.* **2020**, *27*, 12376–12385. DOI: https://doi.org/10.1007/s11356-020-07829-x

[39] M. Rovira, J. Giménez, M. Martínez, X. Martínez-Lladó, J. de Pablo, V. Martí, L. Duro, *J. Hazard. Mater.* **2008**, *150 (2)*, 279–284. DOI: https://doi.org/10.1016/j.jhazmat.2007.04.098

[40] M. Kosmulski, *Surface Charging and Points of Zero Charge*, CRC, Boca Raton, FL **2009**.

[41] T. Missana, U. Alonso, A. C. Scheinost, N. Granizo, M. García-Gutiérrez, *Geochim. Cosmochim. Acta* **2009**, *73 (20)*, 6205–6217. DOI: https://doi.org/10.1016/j.gca.2009.07.005

[42] K. Kalaitzidou, A. A. Nikoletopoulos, N. Tsiftsakis, F. Pinakidou, M. Mitrakas, *Sci. Total Environ.* **2019**, *687*, 1197–1206. DOI: https://doi.org/10.1016/j.scitotenv.2019.06.174

[43] M. Martínez, J. Giménez, J. De Pablo, M. Rovira, L. Duro, *Appl. Surf. Sci.* **2006**, *252 (10)*, 3767–3773. DOI: https://doi.org/10.1016/j.apsusc.2005.05.067

[44] C. A. R. Silva, X. Liu, F. J. Millero, *J. Solution Chem.* **2002**, *31 (2)*, 97–108. DOI: https://doi.org/10.1023/A:1015275618138

[45] *Surface Complexation Modeling: Hydrous Ferric Oxide* (Eds: D. A. Dzombak, F. M. M. Morel), John Wiley & Sons, New York **1990**.

[46] H. Guo, D. Stüben, Z. Berner, *Appl. Geochem.* **2007**, *22 (5)*, 1039–1051. DOI: https://doi.org/10.1016/j.apgeochem.2007.01.004

[47] S. Rakshit, C. J. Matocha, M. S. Coyne, *Soil Sci. Soc. Am. J.* **2008**, *72 (4)*, 1070–1077. DOI: https://doi.org/10.136/sssaj2007.0296